Automated UV-Epoxy-Based Micro-Optic Assembly for Kilowatt-Class Laser-Diode Arrays and Modules

Greg W. Charache, *Senior Member, IEEE*, Furui Wang, Diana Negoita, Faraz Hashmi, Ryan Lanphear, Richard Duck, Juan Ruiz, Bharath Molakala, Joveria Baig, Scott Licari, Tobias Barnowski, Ulrich Bonna, and Hagen Zimer

***Abstract*— This paper outlines the numerous interdisciplinary activities required to implement two ultraviolet (UV) epoxy-based automated micro-optic assembly tools within a "smart factory" for high-power semiconductor laser manufacturing. After a brief overview of the motivation and approach, two examples of automated micro-optic assembly tools [e.g., fast-axis collimation (FAC) lens attach and mirror stripe alignment] for kilowatt-class laser-diode arrays and modules are given that demonstrate the breadth of automation activities required within a modern factory. For each system, the complete assembly sequence is outlined, and the steps that presented fully automated challenges are highlighted. In contrast, to the previous published results that focused on the details of the automated micro-optic alignment, the largest challenges primarily involved automation and repeatability of the UV-epoxy dispense and attach processes for these high-power semiconductor devices. These were solved by precise and stable mechanical design, customized lighting, and machine vision solutions. Finally, the complete integration of the tools into a "smart-factory" system is outlined.**

***Index Terms*— Computer-aided manufacturing, computer vision, diode lasers, manufacturing automation, micro-optics, power lasers, pump lasers, robotics and automation, semiconductor laser arrays, smart factory.**

I. Introduction

THERE has been much discussion in the literature and popular press recently about the increased level of interaction between the factory floor, information technology, and automation. Referred to as Industry 4.0, Digital Transformation, Industrial Internet of Things (IIoT), Internet 4.0, Cyber-Physical Systems, Big Data Analytics, Industrial Value Chain Initiative, e-factory, or Smart Factories, all these projects/programs highlight the increased interconnection between classic manufacturing and numerous information/automation technologies utilized to increase the productivity of various phases of the production process [1]–[7]. It has been observed that <25% of companies are sufficiently interconnected enough to begin this integration, and only 4% of companies produce products with these interconnected machines [8]. In this paper, automation may include both semiautomated as well as fully automated tasks, as demonstrated by a McKinsey study that estimated that 60% of all occupations have ∼30% automatable activities [9].

This paper details two examples of automated micro-optic assembly within a "smart-factory" environment for the manufacturing of high-power (kilowatt-class) semiconductor lasers and modules. There has been much written about the motivation for implementing a "smart factory" including the following: improved productivity, quality, equipment up-time, on-time delivery; and reduced cycle time, rework, scrap, and new process introduction time. In addition, the smart factory promises to relieve workers from harsh/dangerous work environment and allows the integration of development, engineering, production, material resource planning, controlling, and purchasing groups. The smart factory also facilitates: paperless line control and autovalidation; integration of both batch and single-piece product flow; cross-company ordering interface; and supplier interface portal for material order confirmation and forecast.

These goals apply equally well to the manufacturing of high-power semiconductor laser diodes. As with any industry, there are many challenges when trying to implement a "smart factory." In particular, semiconductor laser manufacturing involves highly interdisciplinary activities, including: optical, electrical, mechanical, chemical, and industrial engineering; and robotics, physics, statistics, computer science, and information technology.

However, there are also many enablers that have contributed to the recent push for advanced automation, including: low-cost computing power, vision-guided robotics technology, and machine vision; numerous "powerful" commercial off-the-shelf (COTS) technologies available for system integration; commercialization of "mesoscale" robotic assembly; precision optomechanics to simplify and enable highly repeatable alignment; and the drive to bring back jobs with competitive labor rates.

The approach taken here is to automate as many factory "processes" as possible, including: development, engineering, production, maintenance, purchasing, and accounting. In each of these areas, manual tasks are sought to be eliminated and replaced with cost-effective automation solutions. In our case, this is accomplished by utilizing COTS technology as much as possible (including a scalable platform approach for

Manuscript received December 17, 2018; revised March 5, 2019; accepted March 6, 2019. Date of publication March 8, 2019; date of current version October 17, 2019. Recommended for publication by Associate Editor F. Shi upon evaluation of reviewers' comments. *(Corresponding author: Greg W. Charache.)*

The authors are with TRUMPF Photonics Inc., Cranbury, NJ 08512 USA (e-mail: greg.charache@trumpf.com).

Color versions of one or more of the figures in this article are available online at http://ieeexplore.ieee.org.

Digital Object Identifier 10.1109/TCPMT.2019.2904016

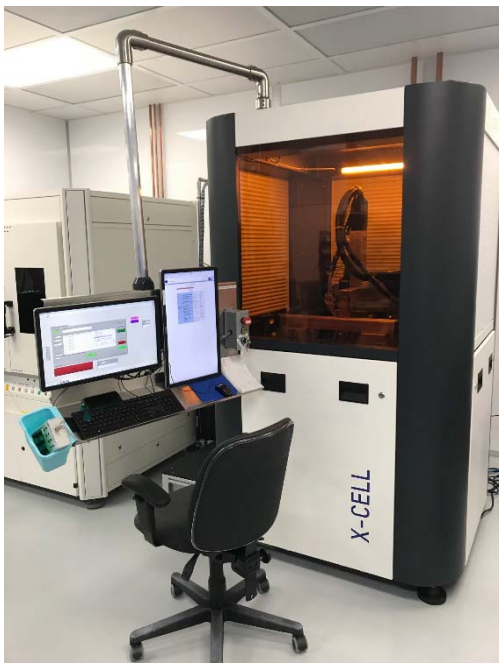

Fig. 1. Automation cell enclosure.

major information-technology components), outsourcing well-defined projects to automation integrators, and using in-house resources for custom integration/software development when requirements are not well defined or likely to need modification. The International Society of Automation includes five levels of automation within a generic "cyber-physical system" [5]:

Level 0: The actual physical process.
Level 1: Activities involved in sensing and manipulating the physical process.
Level 2: Define the activities for monitoring and controlling the physical processes [e.g., structured query language (SQL) database].
Level 3: Define the activities of the workflow to produce the desired end product [e.g., manufacturing execution system (MES)].
Level 4: Define the business-related activities needed to manage an engineering organization [e.g., enterprise resource planning (ERP) system].

It must be emphasized that "automation" is possible at all levels within this smart factory as well as all interconnection points. In the two cases outlined below, emphasis is placed on Levels 0–2. The details of the automated tool integration with Levels 3 and 4 will be detailed in a subsequent publication.

Several semiautomated/fully automated micro-optic assembly systems have been developed in-house for the assembly of TRUMPF Photonics Inc. laser-diode modules (Fig. 1). These systems have many features of previously published systems [10]–[24]; however, these systems are more fully integrated into the overall smart-factory system. Automated micro-optic assembly systems have focused on two attachment technologies: epoxy [15]–[20] and solder [21]–[24]. The two systems [fast-axis collimation (FAC) and mirror stripe alignment] described below in detail are ultraviolet (UV) epoxy-based systems. Both systems feature "active alignment" of

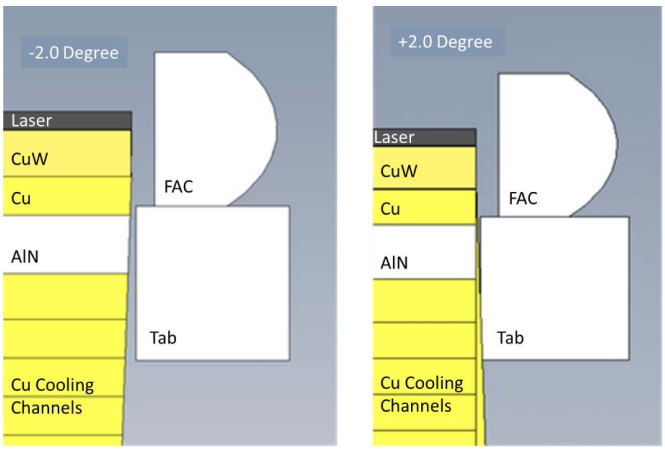

Fig. 2. Cross-sectional schematic of FAC lens/insulated cooler/laser system illustrating the effect of ±2° Cooler front-surface angular tolerance.

an optical element where the laser is activated with a low-duty-cycle (0.1%) high-current pulse generator and the emitted light is captured with a high-resolution CMOS/machine vision camera. It was found that continuous-wave (CW) alignment (and therefore water cooling) was not necessary for optimal alignment for either station. The robot will actively align the optical element to a predefined calibrated target before it is cemented in place with a UV epoxy. As pointed out by others [15]–[20], epoxy selection is a key component to a successful process, and care must be given to select an epoxy that has minimal shrinkage and repeatable batch-to-batch viscosity. Typically, a glue gap of 50 ± 10 μm is targeted, which allows for tolerance compensation with a variable glue gap.

Other features that are common to both systems include the following.

1) Interlocked light-tight enclosure for both laser and robot safety.
2) Separate bottom compartment for housing.
   a) Integrated panels for Deutsches Institut für Normung-rail mounting of electronic/pneumatic components.
   b) Standard 19-in rack mounts for test equipment.
   c) Cable feedthroughs on each of the four corners of the tool.
3) Red-LED-based lighting to enhance automated vision detection algorithms.
4) Integrated high-efficiency particulate air filter to minimize particles within the enclosure. This is very important for kilowatt-class devices.
5) Automated device/module data matrix code reader.
6) Four-axis (x-, y-, z-, and z-axis rotation) pick-and-place Scara robot with ±17-μm placement accuracy.
7) User interface monitors and displays real-time data acquisition. These data are utilized for either fully automated or semiautomated alignment.
8) Optical design yields 0.032-mrad/pixel pointing resolution.
9) Vision-guided pick and place of optical components from Gel-Pak.
10) Automated epoxy processes, including needle position calibration, dispense using a CMOS camera for epoxy

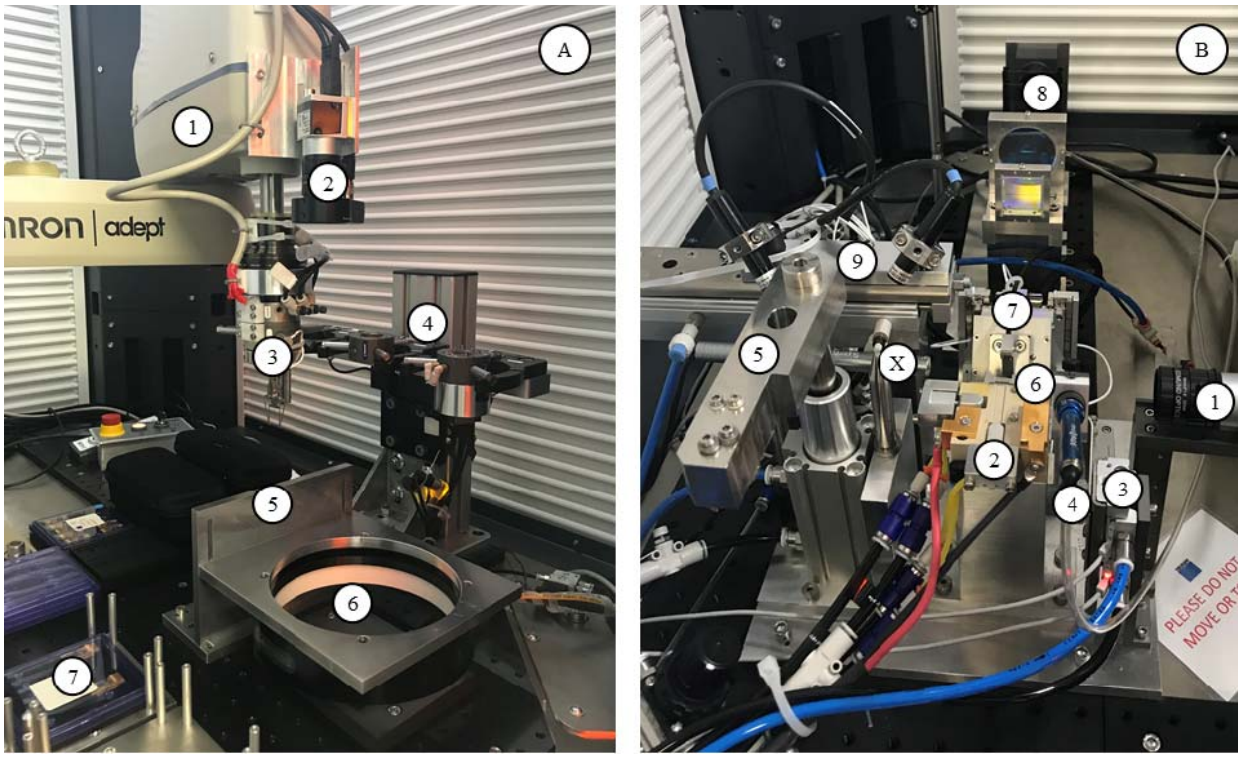

Fig. 3. Fully automated FAC alignment robot: (a) pick and place; (b) six-axis alignment stations.

dot size verification, spread algorithms, and UV-LED cure.

11) LabVIEW/V+ based software development environment.
12) High-reliability COTS electrooptic and linear motion components.
13) 1-in stainless-steel (SS) baseplate for stable optomechanical mounting minimizes vibration.
14) Mechanical design maximizes the use of alignment hard stops, and nonadjustable fixturing maintains high-precision alignment in a 24/7 production environment.

II. FAC Alignment Station

Fig. 2 illustrates a cross-sectional schematic of an FAC/tab assembly aligned to the edge of an insulated microchannel cooler [25] that has a laser bar/CuW-submount attached. This lens serves to collimate the ∼45° full-angle single-mode beam divergence in the vertical direction. Fig. 2 illustrates the tight tolerances needed to maintain a fixed back focal length distance (150 μm) between the FAC lens and the laser array, including the following:

1) laser on submount (i.e., first solder interface);
2) submount on cooler (i.e., second solder interface);
3) angle cut on cooler;
4) FAC on tab.

This fixed distance is maintained by employing a variable (30 $\pm$ 5 μm) epoxy gap and an active alignment process between the FAC/tab assembly with microchannel cooler/submount/laser assembly. Process assembly time, including UV cure, is <5 min per part.

The FAC alignment tool features fully automated 20 independent axes with a 6-degrees-of-freedom (DOF) alignment of an FAC lens for a laser-diode array (CW power ∼0.3 kW) mounted on an insulated microchannel cooler. The process flow is outlined by referring to Fig. 3(a) and (b). For tool setup, there is a seven-position tray manifold that includes the following: input unlensed coolers, output good lensed coolers, output bad lensed coolers, output untested coolers, spare lids, spare trays, and production lids. Initially, an operator will load trays of coolers (A7), sufficient spare empty trays/lids, and a Gel-Pak of FAC lens (A6) into the tool. An epoxy cartridge (B3) is replaced every 100 coolers and/or every shift, and a semiautomated glue-tip position calibration is performed with camera B1.

Once the tool is loaded, the pick-and-place robot (A1) is initiated and picks a cooler from an input tray (A7) and places it on the "test" chuck (B2). In this position, there are two actuators that move the cooler against two alignment hard stops. In this position, the cooler barcode is read with camera A2. This camera includes an autofocus lens to read the laser-marked 2-D barcode on each cooler. Next, the electrical contact is made to the cooler by actuating the contact arm (B5). The robot (A1) then exchanges the cooler pick-up tool with the FAC lens pick-up tool at the tool changer (A4). A lens is picked (mechanical gripper) from the Gel-Pak (A6), the lens is placed on a prealignment hard-stop fixture (B6), and epoxy droplets are applied to the lens (A4). There is also a red-LED ring-light around the Gel-Pak to highlight the edges of each FAC lens to facilitate the vision-guided pick-up tool.

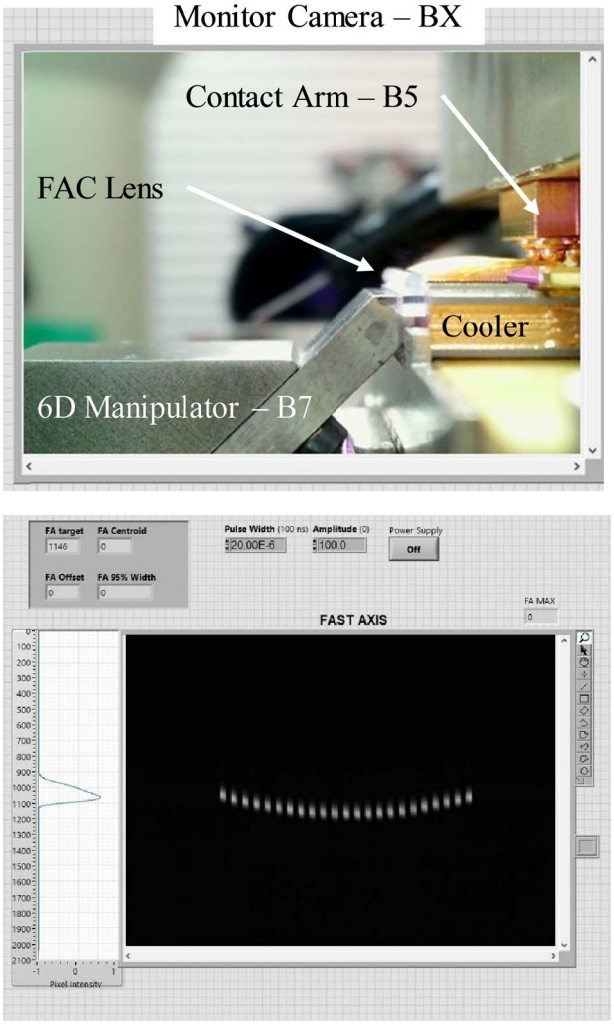

Fig. 4. Screenshot of auto-FAC user interface illustrating the views of camera(s) BX and B8.

Next, the 6-D manipulator (B7) prealigns the lens by pushing it against two hard stops. The lens is then picked up a vacuum pick-up tool on the 6-D manipulator and moves to a preprogrammed prealignment position in front of the laser-diode cooler. The pulsed power supply (100 A, 20 μs, and 0.1% duty cycle) is enabled, and the 6-D manipulator actively aligns the FAC lens such that the centroid of the fast-axis centroid beam points to a predefined target on the camera (B8). Once aligned and the epoxy is evenly spread on the front surface of the cooler, a shield (B3) covers the epoxy glue dispenser (B4) and the UV-LED lights are moved into position for curing (B9). After curing the 6-D manipulator (B7), electrical contact arm (B5), UV lights (B9), cooler alignment actuators (B2), and epoxy shield (B3) move back to their home positions. The robot then picks the cooler and places it in the proper output tray. The sequence repeats until a tray of coolers is completed, and then the robot utilizes a tray tool handler to move empty trays/lids to prepare for the next tray of unlensed devices.

Fig. 4 shows an example screenshot of the user interface illustrating the views of cameras B8 and BX with a properly aligned lens. Camera BX is used by an operator in semiautomated mode to verify the position of the lens relative to

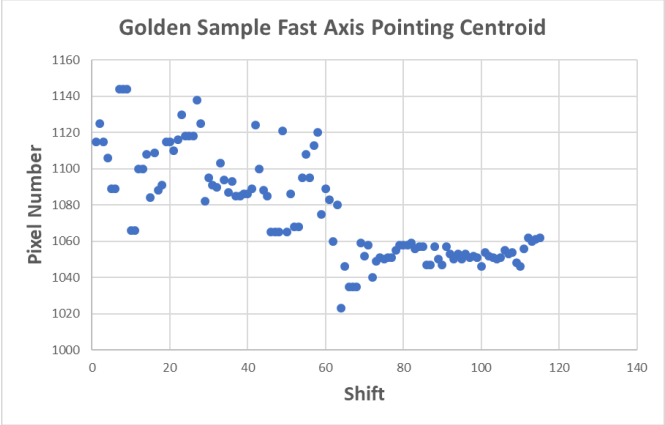

Fig. 5. Golden sample fast-axis pointing centroid stability. Note that a fixture change was instituted to dramatically improve the mechanical stability of the tool after shift 75.

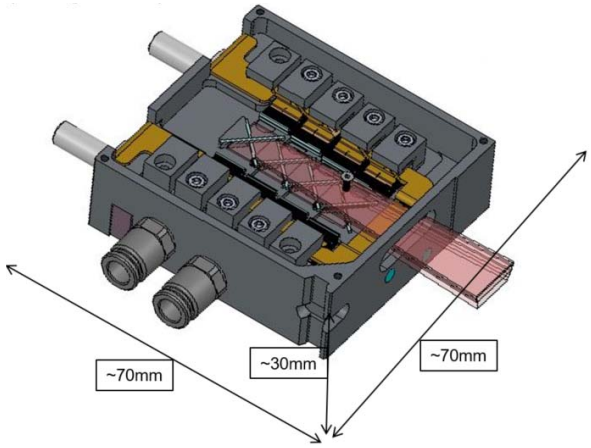

Fig. 6. ~2-kW module design that features eight microchannel coolers on individual vertical steps and eight 90° redirection mirrors.

the insulated microchannel cooler. This screenshot image is uploaded into a shared network directory along with summary process data. Each of these critical process data are determined by quantifying the image data taken by camera B8 and are evaluated against predefined upper and lower specification limits to determine which parts are then placed in pass/fail trays.

The summary process data includes the following:

1) Integrated fast-axis centroid position (e.g., pointing).
2) *Smile:* Difference between the highest and lowest position of each emitters' center of mass.
3) *Tilt Slope/Angle:* Slope and arctangent of emitters' center of mass linear fit.
4) *"Butterfly" Slope/Angle:* Slope and arctangent of emitters' height linear fit (measure of the focus along the length of the array).

These data are transferred to an SQL database for subsequent statistical analysis for process stability. The details of the data transfer protocol, the production database, and the MES system will be detailed in future publication.

Process qualification involved glue-bond shear testing (>1 kgf) and verification of the stability of these parameters after the following environmental stress tests:

1) *High Temperature Stress:* 75 °C and 500 h.

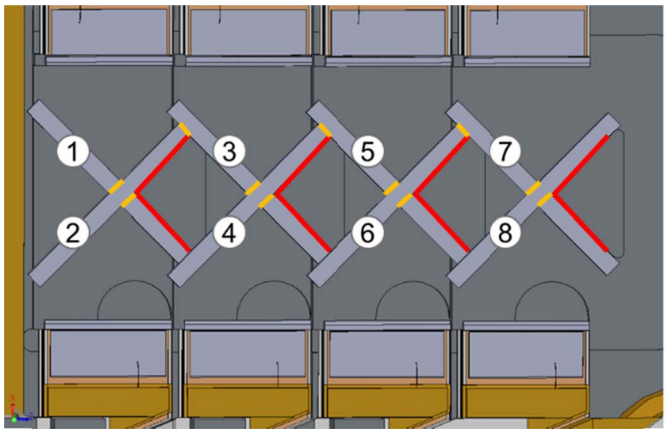

(a)

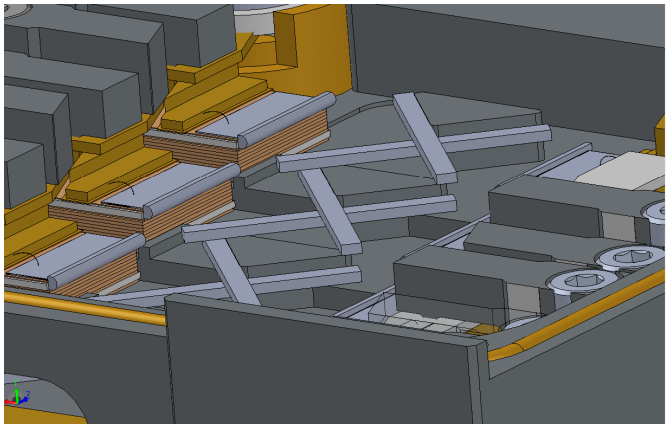

(b)

Fig. 7. (a) Top view of high-power laser module illustrating the mirror attaches process assembly sequence. Attachment is on the backside of mirror stripe opposite of high-reflectivity-coating (see highlighted red), and potential mirror collision areas are highlighted in yellow. (b) 3-D view showing how the mirrors are sequentially attached.

2) *Low Temperature Stress:* −25 °C and 72 h.
3) *Temperature Cycling:* −25 °C–75 °C, 50 cycles, 5 °C/min heating ramp, 2.5 °C/min cooling ramp, dwell time at 75 °C, and −25 °C: 30 min, respectively.
4) *Damp Heat:* 35 °C, 89% RH, and 240 h.

Finally, tool stability is evaluated by checking the pointing of a golden sample before each shift. Example data taken over the course of six months is shown in Fig. 5. Note that a laser-diode clamping fixture change was implemented after shift 75 that dramatically improved the mechanical stability of the system; emphasizing the importance of the overall mechanical design of the tool. The main advantage of moving from a manual to a fully automated process was the increase in the first-pass yield due to improved control of the glue dispense and cure. This resulted in dramatically reduced "hot optics" in subsequent thermal cameral measurements performed during CW testing, which was due to the elimination of glue residue in the laser-diode light path.

III. Mirror Stripe Alignment Station

Fig. 6 illustrates the eight microchannel-cooler laser module designs, where each cooler is passively positioned within a precision machined SS housing at different vertical step heights (e.g., 0.88 mm/step) that enables optical stacking in the fast axis. The coolers placed in this module are the FAC-lensed devices described in Section II. The 90° redirection of collimated coolers inside of the pump module housing is accomplished with high-reflectivity (HR)-coated glass bars

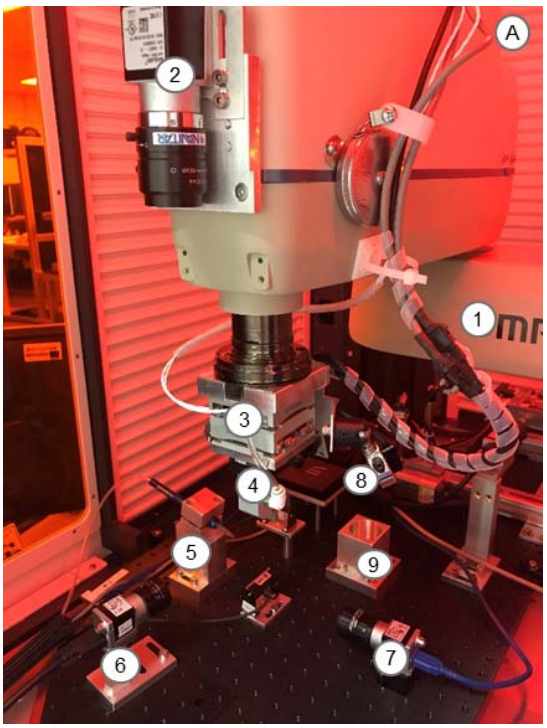

(a)

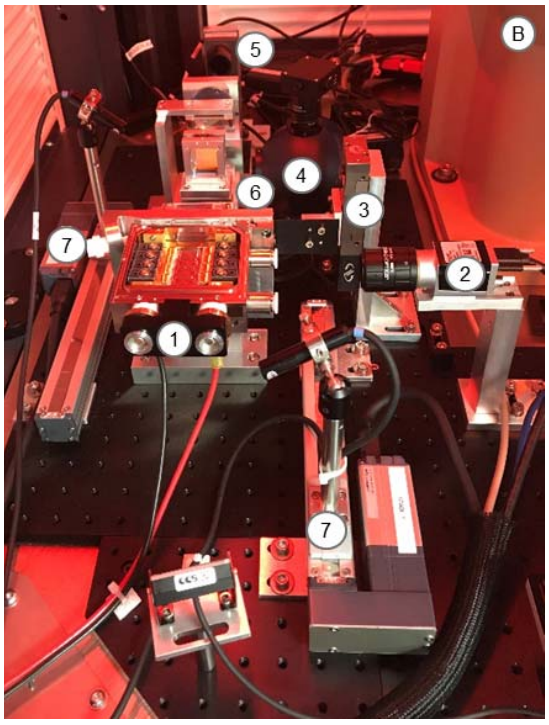

(b)

Fig. 8. Mirror stripe alignment tool: (a) pick-up tool and epoxy dispense; (b) mirror alignment and UV cure.

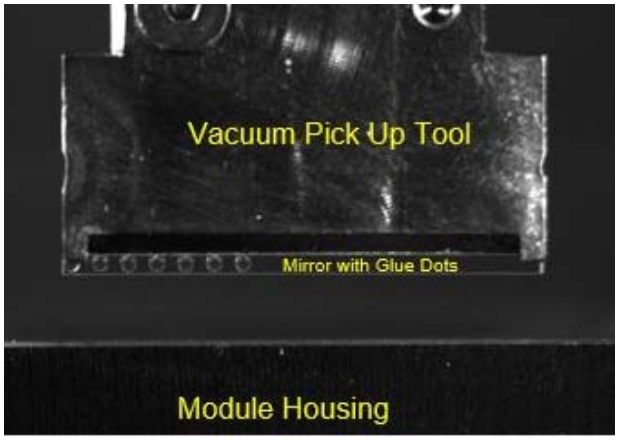

Fig. 9. Image of mirror during leveling procedure.

(mirror stripe) that are UV epoxied to the SS housing. All laser-diode arrays within the module are electrically connected in series. This module is designed for operation up to 300-A CW current and cooling water flow of 8 L/m.

The mirror stripe alignment station features semiautomated 6-DOF alignment of 8× mirrors for this high-power (∼2-kW) laser module. This assembly step aligns the individual mirror stripes ($20 \times 1.5 \times 0.8$ mm^3) for each array and assures the pointing accuracy of each beam in both fast and slow axis. The clear aperture of each mirror measures 18×0.8 mm^2, and the fast axis (FA) beam height is ∼0.6 mm. To achieve the desired FA beam quality, minimizing the tolerance of each of the following parameters is necessary: housing machining, mirror geometry, cooler height, submount height, chip on submount placement, submount on cooler placement, cooler positioning in the housing preassembly, and FAC pointing. As previously mentioned, active alignment with a variable (but stable) glue gap is necessary to compensate for the net effect of all these variable tolerances. Each mirror is actively aligned and attached sequentially, as shown in Fig. 7(a) and (b) with an overall process time of <30 min. Attachment to the housing is accomplished by applying a UV curable epoxy on the backside of the high reflectivity in the red-highlighted regions of Fig. 7(a). When aligning the mirrors, it is necessary to avoid the potential yellow-highlighted collision points in Fig. 7(a).

The overall tool design and process overview can be described by viewing Fig. 8(a) and (b). This tool features nine independent axes and seven process-monitoring cameras. Initially, an operator loads a Gel-Pak tray of mirrors (A8) and activates the vacuum release station. Next, a laser-diode module housing (B1) is loaded into a high-accuracy alignment fixture, and the (+/−) electrical connection is attached. Cooling water is not required as the mirror alignment is performed under a low-duty-cycle (0.1%) pulsed current condition. Finally, epoxy is loaded, the position of the glue tip (A5) is calibrated with cameras (A6/A7) with either an automated or semiautomated algorithm, and all roll-up doors are closed.

The four-axis SCARA robot (A1) uses vision guidance (A2) to pick a mirror from the Gel-Pak (A8) with a vacuum pick-up tool (A4). The SCARA robot then moves to the epoxy dispense station (A5), and multiple drops of epoxy are applied to the

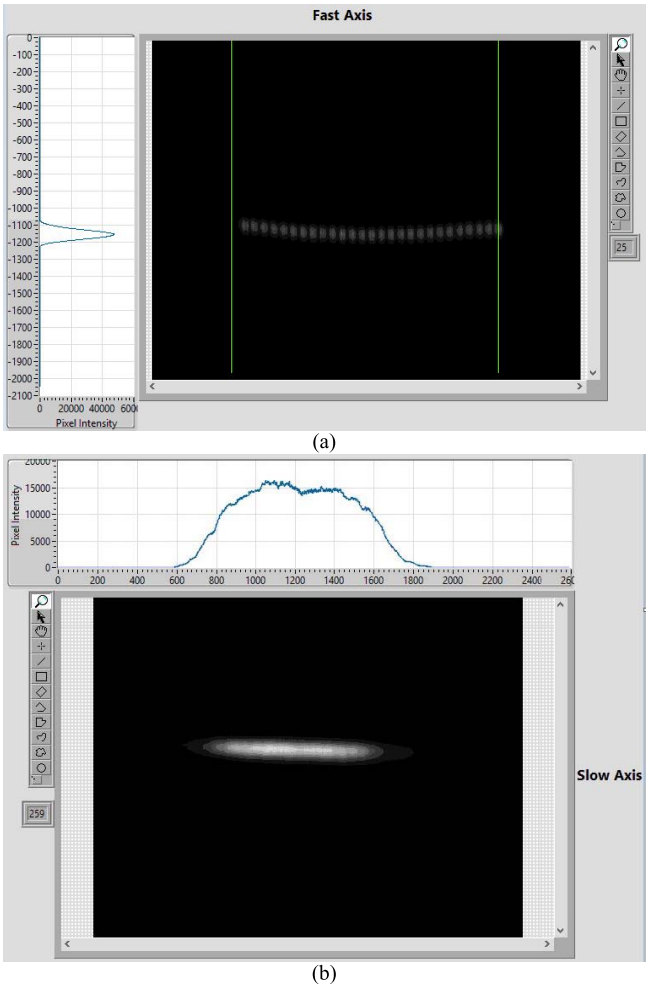

Fig. 10. Example (a) fast-axis far-field and (b) slow-axis near-field images and centroid alignment targets.

mirror stripe opposite the HR-coating. The epoxy droplets are observed with either camera (A7) or an additional camera mounted on the pick-up tool (hidden in this view). After a successful epoxy dispense, the mirror moves on to the mirror leveling camera (B2). Leveling the bottom face of the mirror relative to the module housing is accomplished by one goniometer (A3). At this step, the glue dispense can also be observed (Fig. 9). If the epoxy dispense is not successful, then the mirror is dropped in the scrap bin (A9).

Next, the mirror is moved into a preprogramed prealignment position within the high-power diode laser module (B1). The aperture is adjusted to the correct mirror position (B3), and the pulsed laser power supply (100 A, 20 μs, and 0.1% duty cycle) is then activated and a six-axis alignment (SCARA robot + goniometers) is performed. Initially, the fast-axis far-field pointing (B5) is aligned to a target pixel [Fig. 10(a)], followed by the slow-axis near field (B6) [Fig. 10(b)]. Finally, the z height of the mirror is adjusted with a power-maximizing algorithm using a photodiode mounted on an integrating sphere (B4). These algorithms include exclusion zones to prevent collisions mentioned previously.

The glue spread is observed with camera mounted on the pick-up tool as the mirror is moved toward the SS-housing mount and, subsequently, the mirror is cured in place with

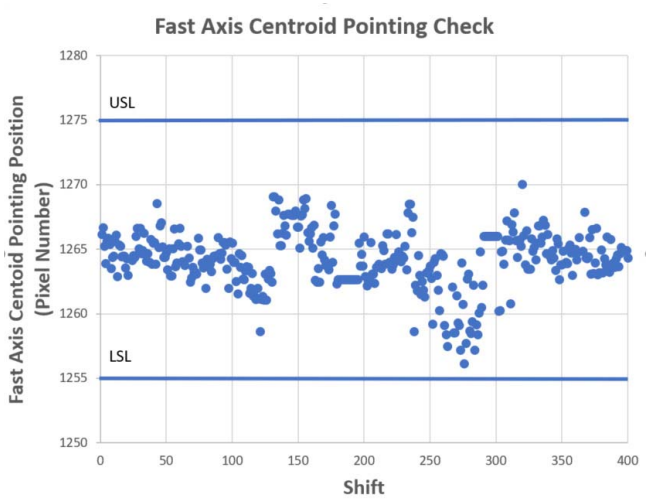

Fig. 11. Golden sample repeatability of the fast-axis centroid pointing for the mirror alignment tool.

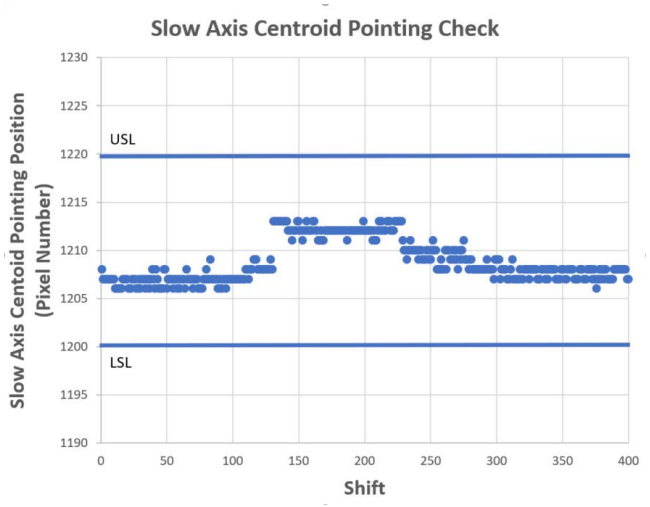

Fig. 12. Golden sample repeatability of the slow-axis centroid pointing for the mirror alignment tool.

the UV lights mounted on separate motion stages (B7). One UV-LED light is used for each side of the module. This process is repeated seven more times to place each mirror stripe within the module. At the end of this sequence, a total beam analysis is performed, and summary process data are uploaded to the SQL database, while the fast-axis far-field and slow-axis near-field images are saved in a separate server. As with the FAC-lensing process data, the summary data along with mirror shear strength are evaluated periodically to establish process stability and control limits.

In addition to the environmental stability tests in Section II, the complete laser-diode module, including the mirror stripes, undergoes the following mechanical stress tests:

1) *Mechanical Shock:* 10 g, 1 ms, 5 cycles/axis, and three axes in total.
2) *Vibration:* 10 g, 20–2000 Hz, 4 min/cycle, 4 cycles/axis, and three axes in total.

Day-to-day tool stability is evaluated by checking the pointing of a golden sample before each shift. Example data taken over the course of six months are shown in Figs. 11 and 12.

IV. Conclusion

This paper highlights many of the diverse technologies and professional disciplines required for the successful integration of automated tools into a smart-factory environment. Two specific examples of micro-optic assembly for kilowatt-class laser-diode arrays are demonstrated, which highlight both the detailed engineering design and data processing requirements for these applications. The development of these automated alignment tools was instrumental in increasing the first-pass yield of these processes to $>95\%$ and significantly reducing scrap and rework costs. In addition, the automated acquisition of process data has led to the rapid identification of process excursions that can now be rectified in a timely manner.

References

[1] D. Pillai, "The future of semiconductor manufacturing," *IEEE Robot. Automat. Mag.*, vol. 13, no. 4, pp. 16–24, Dec. 2006.
[2] Y.-C. Lin *et al.*, "Development of advanced manufacturing cloud of things (AMCoT)—A smart manufacturing platform," *IEEE Robot. Automat. Lett.*, vol. 2, no. 3, pp. 1809–1816, Jul. 2017.
[3] S. Schrauf and P. Berttram. *Industry 4.0: How Digitization Makes the Supply Chain More Efficient, Agile, and Customer-Focused*. [Online]. Available: https://www.strategyand.pwc.com
[4] R. Drath and A. Horch, "Industrie 4.0: Hit or hype?" *IEEE Ind. Electron. Mag.*, vol. 8, no. 2, pp. 56–58, Jun. 2014.
[5] J.-R. Jiang, "An improved cyber-physical systems architecture for industry 4.0 smart factories," in *Proc. IEEE Int. Conf. Appl. Syst. Innov.*, 2017, pp. 918–920.
[6] W. Rong, G. T. Vanan, and M. Phillips, "The Internet of Things (IoT) and transformation of the smart factory," in *Proc. Int. Electron. Symp.*, Sep. 2016, pp. 399–402.
[7] G. Ball, C. Runge, R. Ramsey, and N. Barrett, "Systems integration and verification in an advanced smart factory," in *Proc. Annu. IEEE Int. Syst. Conf. (SysCon)*, Apr. 2017, pp. 1–5.
[8] M. Kurth and C. Schleyer, "Smart Factory and Education," in *Proc. IEEE 11th Conf. Ind. Electron. Appl. (ICIEA)*, 2016, pp. 1057–1061.
[9] J. Bughin *et al.*, "Artificial intelligence: The next digital frontier," McKinsey Global Inst., Tech. Rep., Jun. 2017.
[10] J. Liu *et al.*, "Locating end-effector tips in robotic micromanipulation," *IEEE Trans. Robot.*, vol. 30, no. 1, pp. 125–130, Feb. 2014.
[11] H. Bettahar, A. Caspar, C. Clévy, N. Courjal, and P. Lutz, "Photo-robotic positioning for integrated optics," *IEEE Robot. Automat. Lett.*, vol. 2, no. 1, pp. 217–222, Jan. 2017.
[12] D. O. Popa and H. E. Stephanou, "Micro and meso scale robotic assembly," *J. Manuf. Processes*, vol. 6, no. 1, pp. 52–71, 2004.
[13] X. Ye, J. Gao, Z. Zhang, C. Shao, and P. Liu, "Robotic microassembly for meso-scale application," *Ind. Robot., Int. J.*, vol. 42, no. 2, pp. 142–148, 2015.
[14] J. Hiltner, "Embedded vision finds a role in the IIoT," *Ind. Photon.*, pp. 11–12, Oct. 2017.
[15] J. Miesner *et al.*, "Automated assembly of fast-axis collimation (FAC) lenses for diode laser bar modules," *Proc. SPIE*, vol. 7198, Feb. 2009, Art. no. 71980G.
[16] C. Brecher, N. Pyschny, S. Haag, and V. G. Lule, "Automated alignment of optical components for high-power diode lasers," *Proc. SPIE*, vol. 8241, Feb. 2012, Art. no. 82410D.
[17] T. Müller, S. Haag, D. Zontar, S. Sauer, and C. Brecher, "Customizable assembly solutions for optical systems," in *Proc. High Power Diode Lasers Syst. Conf.*, 2015, pp. 23–24.
[18] S. Haag *et al.*, "Flexible assembly module for beam-shaping product families based on support structures," *Proc. SPIE*, vol. 9727, Apr. 2016, Art. no. 97270W.
[19] S. Sauer, T. Müller, S. Haag, and D. Zontar, "Machine platform and software environment for rapid optics assembly process development," *Proc. SPIE*, vol. 9730, Apr. 2016, Art. no. 973019.
[20] S. Sauer *et al.*, "Individualized FAC on bottom tab subassemblies to minimize adhesive gap between emitter and optics," *Proc. SPIE*, vol. 10086, Feb. 2017, Art. no. 100860U.
[21] J. Miesner, F. Frischkorn, N. Boenig, D. Rose, T. Vahrenkamp, and K. Boucke, "Full automated packaging of high-power diode laser bars," in *Proc. IEEE Electron. Compon. Technol. Conf.*, May 2008, pp. 985–990.

[22] M. Leers *et al.*, "Highly precise and robust packaging of optical components," *Proc. SPIE*, vol. 8244, Feb. 2012, Art. no. 824404.
[23] H. Faidel *et al.*, "Passive alignment and soldering technique for optical components," *Proc. SPIE*, vol. 8235, Feb. 2012, Art. no. 82351I.
[24] M. Leers *et al.*, "Pick and align—High precision active alignment of optical components," in *Proc. IEEE 62nd Electron. Compon. Technol. Conf.*, May 2012, pp. 208–212.
[25] S. Heinemann *et al.*, "Packaging of high-power bars for optical pumping and direct applications," *Proc. SPIE*, vol. 9348, Mar. 2015, Art. no. 934807.

Greg W. Charache (M'87–SM'98) received the B.S. degree from the University of Delaware, Newark, DE, USA, in 1988, and the M.S. and Ph.D. degrees in electrical engineering from the Rensselaer Polytechnic Institute, Troy, NY, USA, in 1991 and 1994, respectively.

From 1994 to 2000, he was a Senior Researcher with Lockheed Martin's Knolls Atomic Laboratory, Schenectady, NY, USA, where he was involved in InP- and GaSb-based thermophotovoltaic devices and systems. In 2000, he joined Princeton Lightwave, Inc., Cranbury, NJ, USA, as a Senior Researcher/Reliability Manager for high-power single-mode ridge waveguide InP-based semiconductor laser diodes used in the telecom industry. In 2002, the company was acquired by the TRUMPF Group, Ditzingen, Germany, for the development and manufacturing of high-power GaAs-based laser diodes for industrial applications. He is currently the Head of the Equipment Development and Automation Group, TRUMPF Photonics Inc., Cranbury, which develops and manufactures high-power GaAs-based multimode laser-diode modules used for industrial manufacturing. At TRUMPF Photonics Inc., he has worked in various roles in both development and production. He has authored over 75 papers and holds 7 patents.

Furui Wang received the B.S. and M.S. degrees in mechanical engineering from the University of Science and Technology of China, Hefei, China, in 2003 and 2006, respectively, and the Ph.D. degree in mechanical engineering from Vanderbilt University, Nashville, TN, USA, in 2011.

From 2011 to 2014, he was a Systems Engineer with Abbott Laboratories, Princeton, NJ, USA. He is currently a Senior Automation Engineer with TRUMPF Photonics Inc., Cranbury, NJ, USA. His current research interests include robotics, automation, and hardware systems integration.

Diana Negoita received the M.S. degree in digital signal processing from Rutgers University, New Brunswick, NJ, USA, in 2016.

She is currently an Automation Engineer with the Equipment Development and Automation Department, TRUMPF Photonics Inc., Cranbury, NJ, USA. Her work focuses on integrating machine vision on automation projects: OCR, image processing for process control: FAC active alignment, near-field emitter count, glue curing inspection, and part alignment. Her current research interests include the integration of deep learning for detection and the classification for visual inspection.

Faraz Hashmi received the B.S. degree in electrical and computer engineering technology from the New Jersey Institute of Technology, Newark, NJ, USA, in 2009.

He is currently an Automation Engineer with the Equipment Development and Automation Group, TRUMPF Photonics Inc., Cranbury, NJ, USA, where he is involved in automation planning, designing, and execution of the processes and implementation of robotics safety.

Ryan Lanphear received the B.S. degree in computer engineering from Drexel University, Philadelphia, PA, USA, in 2018.

He is currently an Automation Engineer with TRUMPF Photonics Inc., Cranbury, NJ, USA, where he is involved in process cycle time, robotic path planning, and system integration techniques.

Richard Duck was with AT&T/Lucent Technologies, Holmdel, NJ, USA, from 1987 to 1999, working on the mechanical layout and design of telephone switching equipment and also the design of submarine cable equipment for the group that later became TE Connectivity, where he became certified as an ISO9000 Lead Assessor/Auditor. From 2000 to 2006, he was a Lead Mechanical Designer with the Amplifier Division, JDS Uniphase, Ewing, NJ, USA, and a Key Member of the design of the OA series erbium-doped fiber amplifiers (EDFAs). He has extensive experience in the design of fixturing and automated tooling used in the development and production of diode lasers. Since 2007, he has been a Senior Mechanical Design Engineer with TRUMPF Photonics Inc., Cranbury, NJ, USA. His credits also include experience in the manufacturing field as an employee of Safran Aerosystems (Air Cruisers), Wall, NJ, USA, and Ocean Power Technologies, Pennington, NJ, USA.

Juan Ruiz received the B.S. degree in material science and engineering from Rutgers University, New Brunswick, NJ, USA, in 2001.

He was an Epitaxy/Growth Engineer with Princeton Lightwave, Inc., Cranbury, NJ, USA, manufacturing high-power InP-based semiconductor laser diodes used in the telecom industry. In 2002, he joined the TRUMPF Group, Ditzingen, Germany, where he focused on wafer processing (photolithography, etching, electroplating, and wafer thinning) of high-power GaAs-based laser diodes for industrial applications. In 2014, he became the Group Lead of the Diode Lasers Assembly Engineering Group, TRUMPF Photonics Inc., Cranbury which included: flip-chip bonding, wire bonding, electro-optical testing, and lensing and assembly processes. He has extensive experience in process integration and new product introduction for both wafer fab and back-end assembly processes. He is currently the Engineering Manager of the Diode Lasers Packaging, Lensing, Testing and Assembly Group, TRUMPF Photonics Inc. He is involved in process control, sustaining, and continuous improvement using lean manufacturing and six-sigma techniques.

Bharath Molakala received the B.S. degree in electrical and electronics engineering from Sri Venkateshwara University, Tirupati, India, in 2012, and the M.S. degree in electrical and computers engineering from Rutgers University, New Brunswick, NJ, USA, in 2016.

In 2015, he joined TRUMPF Photonics Inc, Cranbury, NJ, USA, as an Automation Engineer Co-op and worked on process automation of testing, lensing, and assembly of diode lasers. From 2016 to 2018, he was a Process Engineer of testing and lensing of laser diodes with TRUMPF Photonics Inc., where he worked on process and yield improvements, troubleshooting, and cycle time reduction by automating the processes. He is currently an Equipment Integration Engineer with TRUMPF Photonics Inc., where he works on the integration of new equipment into the production line.

Joveria Baig received the B.S degree in electrical engineering from the Lahore University of Management Sciences, Lahore, Pakistan, in 2012, and the Erasmus Mundus Double Masters with the M.Sc. degree in applied physics from TU Delft, Delft, Netherlands, and the M.Sc. degree in laser optics and matter from the Institut d'Optique Graduate School, Palaiseau, France, and the University of Oxford, Oxford, U.K., in 2014.

In 2015, she joined the Tyndall National Institute, University College Cork, Cork, Ireland, as a Ph.D. Researcher, where her research focused on design, fabrication, and characterization of InP-based integrated tunable lasers for burst mode transmitters, as a part of the EU Mode Gap Project until 2016. She is currently a Lensing Engineer with TRUMPF Photonics Inc., Cranbury, NJ, USA, where she supports lensing processes involved in the manufacturing of high-power laser modules. She is involved in various outreach efforts to promote science among women.

Ms. Baig has represented Ireland as a "Change Maker" in the IEEE Women at the Engineering International Leadership Conference. She was a twice recipient of the SPIE Optics and Photonics Scholarship.

Scott Licari born in 1995. He received the B.S. degree in electrical engineering with a focus in optics, optical components, Fourier optics, and holography from the School of Electrical Engineering, Pennsylvania State University, University Park, PA, USA, in 2017.

He has been a Lensing Engineer with TRUMPF Photonics Inc., Cranbury, NJ, USA, where he has supported many projects regarding fully automated and semiautomated systems in the production of high-power (class-4) lasers.

Tobias Barnowski received the Dipl.-Ing. degree in laser engineering from the Münster University of Applied Science, Münster, Germany, in 2002.

He finished his Diploma dissertation at Jenoptik L.O.S., Jena, Germany. He was with Trumpf Laser GmbH, Schramberg, Germany, for five years, as a Trouble Shooter in the production of multi-kilowatt solid-state lasers as well as in the field service in the industrial environment. After collecting experience about the conditions in which high-power lasers for welding and cutting are used in the sheet metal industry, he changed into the product development at TRUMPF Photonics Inc., Cranbury, NJ, USA, in 2008, where he has been the Group Leader since 2018. His focus is cost reduction and performance improvement of pumps for the TruDisk Systems as well as for highly innovative ultrashort pulse lasers in a competitive industrial market.

Ulrich Bonna received the Dipl.-Ing. degree in mechanical engineering from the University of Furtwangen, Furtwangen, Germany, in 1989.

He was a Mechanical Design Engineer with the Opto-Electronics Industry. In 1999, he joined TRUMPF Laser GmbH, Schramberg, Germany, as a Solid-State Laser Designer. In 2005, he joined TRUMPF Photonics Inc., Cranbury, NJ, USA, as the Head of the Mechanical Design Department. In 2009, he was with the Packaging and Assembly Production Department, TRUMPF Photonics Inc.

Hagen Zimer received the Diploma degree in applied physics from the Münster University of Applied Science, Münster, Germany, in 1998, and the Doctorate degree from Friedrich-Schiller University Jena, Jena, Germany, in 2006.

From 2005 to 2007, he was with TRUMPF Lasermarking Systems AG, Grüsch, Switzerland, where he developed novel industrial diode-pumped solid-state lasers for laser marking applications. From 2007 to 2011, he was the Head of the High-Power Fiber Laser Group, JT Optical Engine GmbH, Jena, a Jenoptik-TRUMPF joint venture, where he was the Head of the fundamental research of short-pulsed and multi-kilowatt continuous-wave fiber lasers and the related development of fiber optic high-power components. In 2013, he established and led a new Research and Development Group, TRUMPF, with the goal to develop novel direct diode lasers based on spectral beam combining to target multi-kilowatts of output power for high-brightness laser applications. From 2016 to 2018, he was the Head of the Research and Development Department, TRUMPF's Diode Laser Facility, Cranbury, NJ, USA. He became the Managing Director and the CEO of that site in 2018, where has been responsible for TRUMPF's diode laser product portfolio. He has over 17 years of experience in the field of high-power solid-state laser engineering. He is currently the President and the CEO of TRUMPF Photonics Inc., Cranbury, NJ, USA. His scientific and industrial expertise spreads over a broad range of solid-state laser platforms such as diode-pumped rod and fiber lasers, slab lasers, thin disk lasers, and broad-area diode lasers. He has authored more than 50 papers. He is the (Co-)Inventor of 11 patents.

Dr. Zimer has contributed to several conferences and gave invited talks on high-power fiber lasers, high-power processing optics, and ultrahigh-brightness diode lasers.